BJP BRITISH JOURNAL OF PHARMACOLOGY

BPS BRITISH PHARMACOLOGICAL SOCIETY

British Journal of Pharmacology (2009), 158, 621–632

0007-1188/09
www.brjpharmacol.org

RESEARCH PAPER

Characteristic changes in coronary artery at the early hyperglycaemic stage in a rat type 2 diabetes model and the effects of pravastatin

J Kajikuri, Y Watanabe, Y Ito, R Ito, T Yamamoto and T Itoh

Department of Pharmacology, Graduate School of Medical Sciences, Nagoya City University, Nagoya, Japan

Background and purpose: Diabetes is a risk factor for the development of coronary artery disease but it is not known whether the functions of endothelium-derived nitric oxide (NO) and endothelium-derived hyperpolarizing factor (EDHF) in coronary arteries are altered in the early stage of diabetes. Such alterations and the effects of pravastatin were examined in left anterior descending coronary arteries (LAD) from Otsuka Long-Evans Tokushima Fatty (OLETF) rats (type 2 diabetes model) at the early hyperglycaemic stage [vs. non-diabetic Long-Evans Tokushima Otsuka (LETO) rats].
Experimental approach: Isometric tension, membrane potential and superoxide production were measured, as were protein expression of NAD(P)H oxidase components and endothelial NO synthase (eNOS).
Key results: Superoxide production and the protein expressions of both the nicotinamide adenine dinucleotide (phosphate) [NAD(P)H] oxidase components and eNOS were increased in OLETF rats. These changes were normalized by pravastatin administration. Not only acetylcholine (ACh)-induced endothelial NO production but also functions of endothelium-derived NO [from (i) the absolute tension induced by epithio-thromboxane A_2 (STA_2) or high K^+; (ii) enhancement of the STA_2-contraction by a nitric oxide synthase (NOS) inhibitor; and (iii) the ACh-induced endothelium-dependent relaxation of high K^+-induced contraction] or EDHF [from (iv) ACh-induced endothelium-dependent smooth muscle cell hyperpolarization and relaxation in the presence of a NOS inhibitor] were similar between LETO and OLETF rats [whether or not the latter were pravastatin-treated or -untreated].
Conclusions and implications: Under conditions of increased vascular superoxide production, endothelial function is retained in LAD in OLETF rats at the early hyperglycaemic stage, partly due to enhanced endothelial NOS protein expression. Inhibition of superoxide production may contribute to the beneficial vascular effects of pravastatin.
British Journal of Pharmacology (2009) **158,** 621–632; doi:10.1111/j.1476-5381.2009.00348.x; published online 23 July 2009

Keywords: Coronary artery; endothelium-derived hyperpolarizing factor; endothelium-derived nitric oxide; pravastatin; type 2 diabetes; superoxide; endothelial nitric oxide synthase; hyperglycaemia

Abbreviations: Ang II, angiotensin II; AT_1R, angiotensin type 1 receptor; DAF-2, diaminofluorescein-2; EDHF, endothelium-derived hyperpolarizing factor; EDRF, endothelium-derived relaxing factor; HbA1c, glycated haemoglobin A1c; HMG-CoA, 3-hydroxy-3-methylglutaryl coenzyme A; HOMA-IR, homeostasis model assessment of insulin resistance; L-012, 8-amino-5-chloro-7-phenylpyridol[3,4-d]pyridazine-1,4-(2H,3H)dione sodium salt; LAD, left anterior descending coronary artery; LETO, Long-Evans Tokushima Otsuka; L-NAME, N^{ω}-nitro-L-arginine methyl ester; L-NNA, N^{ω}-nitro-L-arginine; OLETF, Otsuka Long-Evans Tokushima Fatty; PEG-SOD, polyethylene glycol-superoxide dismutase; STA_2, 9,11-epithio-11,12-methano-thromboxane A_2

Introduction

The endothelium plays key roles in the regulation of vascular tone and in the development of atherosclerosis through the synthesis and release of endothelium-derived relaxing factors (EDRFs) [such as nitric oxide (NO), prostacyclin and endothelium-derived hyperpolarizing factor (EDHF)] (Quyyumi, 1998; De Vriese *et al.*, 2000). Indeed, in the regulation of coronary artery vasomotor function, NO and EDHF are thought to play central roles (Kugiyama *et al.*, 1997; De Vriese *et al.*, 2000). It has been demonstrated that endothelial dysfunction is an independent predictor of adverse cardiovascular events in humans (Halcox *et al.*, 2002) and that diabetes is an important risk factor for the development of coronary artery disease (Kannel and McGee, 1979). In fact, it has been estimated that among diabetic patients, 75% of deaths may be attributable to coronary artery disease (Bonow *et al.*, 1996).

Correspondence: Takeo Itoh, Department of Pharmacology, Graduate School of Medical Sciences, Nagoya City University, Nagoya 467-8601, Japan. E-mail: titoh@med.nagoya-cu.ac.jp
Received 13 March 2009; accepted 8 April 2009

It is thought that in several animal models of type 1 or type 2 diabetes, the elevated blood glucose level leads to an increase in vascular superoxide production, thus causing a dysfunction of endothelium-derived NO in conduit arteries (for review, see De Vriese *et al.*, 2000). However, whether a dysfunction of endothelium-derived NO and/or EDHF in coronary arteries has already developed at the early hyperglycaemic stage in type 2 diabetes remains to be clarified. The Otsuka Long-Evans Tokushima Fatty (OLETF) rat, an established model of human type 2 diabetes, is characterized by having the following: insulin-resistance from 12 weeks of age, late-onset hyperglycaemia (after 20 weeks of age) and a reduced insulin level from 60 weeks of age (Kawano *et al.*, 1992). Previous comparisons with its normal counterpart [the non-diabetic Long-Evans Tokushima Otsuka (LETO) rat] have shown that the functions of both endothelium-derived NO and EDHF are reduced in the aorta (Nakamura *et al.*, 2001) and in the mesenteric artery (Minami *et al.*, 2002) of OLETF rats, although whether this is also true of the coronary arteries remains to be clarified.

Pravastatin, an inhibitor of 3-hydroxy-3-methylglutaryl coenzyme A (HMG-CoA) reductase, reduces adverse cardiovascular events and retards the development of diabetes in male humans with hypercholesterolaemia (Shepherd *et al.*, 1995; Freeman *et al.*, 2001). However, the mechanism underlying this important action of pravastatin remains to be fully clarified. Beneficial effects of pravastatin on adverse cardiovascular events have also been demonstrated in OLETF rats following its continuous administration from 5–6 weeks of age (pre-insulin-resistance stage) (Yu *et al.*, 2004; Chen *et al.*, 2007). However, nothing is known about its effects on endothelium-derived NO and EDHF in the coronary artery in OLETF rats when it is administered *after* hyperglycaemia has developed.

To try to clarify the above issues, we investigated: (i) whether the functions of endothelium-derived NO and EDHF and/or vascular superoxide production are abnormal in the left anterior descending coronary artery (LAD) of OLETF rats at the early hyperglycaemic stage (vs. age-matched LETO rats) and (ii) whether pravastatin has beneficial effects on the coronary artery when this agent is chronically administered *in vivo* after hyperglycaemia has developed.

Methods

Animals

All experiments performed in this study conformed to Guidelines on the Conduct of Animal Experiments issued by the Graduate School of Medical Sciences in Nagoya City University and were approved by the Committee on the Ethics of Animal Experiments in that institution. Male OLETF rats and LETO rats (genetic control for OLETF rats) were obtained from Tokushima Research Institute, Otsuka Pharmaceutical Co. (Tokushima, Japan). The rats were fed standard laboratory chow and given tap water *ad libitum*. From 20 weeks of age, some of the OLETF rats were given pravastatin (100 $mg \cdot kg^{-1} \cdot day^{-1}$) (Yu *et al.*, 2004) for 8 weeks in their drinking water. The rats were used in the present study at 28 weeks of age. Systolic blood pressure was measured in conscious rats by tail-cuff plethysmography. For the measurement of blood glucose concentrations, blood samples were collected via the tail vein from overnight-fasted rats before and at 30, 60 and 120 min after oral glucose (2 $g \cdot kg^{-1}$) administration ('oral glucose tolerance test').

After an overnight fast, rats were anaesthetized with sevoflurane and killed by exsanguination. Blood samples were collected for the determination of the concentrations of fasting blood glucose, glycated haemoglobin A1c (HbA1c), serum insulin and plasma, nitrite/nitrate (NOx).

Tissue preparation

The heart was immediately excised and placed in Krebs solution, and the LAD (outer diameter, 0.15–0.30 mm) was then isolated and cleaned. A segment of each artery was cut open along its long axis (using small scissors), and circularly cut strips were prepared using a small razor blade, as described previously (Itoh *et al.*, 1992; Kusama *et al.*, 2005b; Watanabe *et al.*, 2008). In some preparations, the endothelium was removed by gently rubbing the intimal surface of the strips with small pieces of razor blade (Itoh *et al.*, 1992).

Isometric tension measurement

Using the circularly cut strips (0.7–0.8 mm long, 0.25 mm wide), isometric tension was measured as described previously (Itoh *et al.*, 1992; Kusama *et al.*, 2005b; Watanabe *et al.*, 2008). The resting tension was adjusted to obtain maximum contraction in high-K^+ solution (128 mM). Guanethidine (5 μM, to prevent effects due to release of sympathetic transmitters) and diclofenac (3 μM, to inhibit the production of cyclooxygenase products) were present throughout the experiments.

Endothelium-dependent relaxation was induced by ACh during the contraction induced by 40 mM K^+ or 30 nM 9,11-epithio-11,12-methano-thromboxane A_2 (STA_2). Each preparation was first contracted with 40 mM K^+ or 30 nM STA_2. Then, after a steady-state contraction had been attained, ACh (10^{-9}–10^{-6} M) was cumulatively applied from low to high concentration (for 2 min at each concentration) during the ongoing contraction. To examine the effects of nitric oxide synthase (NOS)-inhibition, the tissues were pretreated with N^{ω}-nitro-L-arginine (L-NNA; 0.1 mM) for 60 min and this was present throughout the experiments.

After the control response to ACh had been recorded, polyethylene glycol-superoxide dismutase (PEG-SOD, 100 $u \cdot mL^{-1}$) together with catalase (400 $u \cdot mL^{-1}$) was applied for 30 min in Krebs solution, and ACh (10^{-9}–10^{-6} M) was again cumulatively applied during the contraction induced by 40 mM K^+ in the presence of PEG-SOD + catalase.

Electrophysiological study

Membrane potentials were measured in smooth muscle cells using a conventional microelectrode technique, as described previously (Kusama *et al.*, 2005a; Watanabe *et al.*, 2008). The effects of L-NNA with or without charybdotoxin (a blocker of intermediate- and large-conductance Ca^{2+}-activated K^+ channels) plus apamin (a blocker of small-conductance Ca^{2+}-activated K^+ channels) (Garland *et al.*, 1995; Marchenko and Sage, 1996) on the ACh-induced hyperpolarization were

examined as follows. First, ACh (1 μM) was applied for 1 min followed by a 15-min washout (to allow the response to recover), and L-NNA was then applied for 30 min. ACh was again applied followed by a 15-min washout with a solution containing L-NNA. Charybdotoxin (0.1 μM) plus apamin (0.1 μM) were subsequently applied for 3 min in the presence of L-NNA, and ACh was finally applied in the presence of charybdotoxin plus apamin. This series was performed in one and the same strip.

Biochemical analyses

Whole blood was used for measuring glucose and HbA1c concentrations. Blood glucose was measured by the glucose oxidase method using Antsense II, while HbA1c was measured by means of a DCA2000 analyser. The plasma insulin concentration was quantified using a commercially available ELISA insulin kit. From these values, the homeostasis model assessment of insulin resistance (HOMA-IR) score was calculated: insulin ($\mu U \cdot mL^{-1}$) × glucose (mM) being divided by 22.5 (Matthews *et al.*, 1985).

Plasma NOx measurement

Plasma NOx concentrations were measured using a NO analyser, NOA 280, according to a method described previously (Cash *et al.*, 2001).

Measurement of superoxide production

Changes in superoxide production in endothelium-intact strips of LAD (7 mm long) were examined using the superoxide-sensitive chemiluminescent dye 8-amino-5-chloro-7-phenylpyridol[3,4-d]pyridazine-1,4-(2H,3H)dione sodium salt (L-012; 100 μM) and a luminometer, as described previously (Yamamoto *et al.*, 2005; Kikuchi *et al.*, 2008). When the effect of N^{ω}-nitro-L-arginine methyl ester (L-NAME) was to be examined, the strips were pre-incubated for 30 min in N-(2-hydroxyethyl)piperazine-N′-(2-ethanesulfonic acid) (HEPES)-buffered solution with or without L-NAME (3 mM).

Superoxide production was also detected by means of the oxidative fluorescence dye dihydroethidium using a segment of LAD in optimal cutting temperature (OCT) compound, as described previously (Kusama *et al.*, 2005a; Kikuchi *et al.*, 2008). When the effect of L-NAME was to be examined, the sections were pre-incubated in HEPES-buffered solution with or without L-NAME (3 mM). Images were obtained using a confocal-laser-scanning microscope system. The fluorescence intensity in each image was read from eight randomly selected regions (10 × 10 pixels) and averaged using digital image-analyser software.

Measurement of nicotinamide adenine dinucleotide phosphate (NADPH) oxidase activity

Each LAD strip was homogenized, using a glass homogenizer, in 50 mM phosphate buffer containing 1 mM ethyleneglycol bis (2-aminoethylether)-N,N,N′,N′,-tetraacetic acid (EGTA) and protease inhibitors. The assay was performed in 50 mM phosphate buffer, pH 7.0, containing 1 mM EGTA, 0.15 M sucrose, 0.1 mM L-012 and 0.1 mM NADPH as the substrate. The NADPH oxidase activities were measured according to a method described previously (Bayraktutan *et al.*, 1998).

$[NO]_i$ measurement

The intracellular concentration of NO ([NO]i) within endothelial cells was estimated from the change in the fluorescence intensity of the nitric-oxide-sensitive dye diaminofluorescein-2 (DAF-2), as described previously (Yamamoto *et al.*, 2005). In brief, endothelium-intact strips were exposed to membrane-permeable DAF-2 diacetate (10 μM) in Krebs solution, then washed with Krebs solution for 10 min. DAF-2 was excited at 490 nm at 30-s intervals and the DAF-2 fluorescence intensity within endothelial cells at any given time after the application of ACh (F) was normalized with respect to the fluorescence intensity measured just before the application of ACh (F_0) in the same experiment. Thus, changes in $[NO]_i$ are expressed as F/F_0. The mean fluorescence intensities obtained from five endothelial cells in each strip were averaged and this value (one value per strip) was used for the later analysis.

Immunohistochemical staining

A frozen segment of LAD embedded in OCT compound was cut at 6 μm thickness on a cryostat, then mounted on MAS-coated glass slides. The sections were incubated overnight at 4°C with anti-endothelial NO synthase (eNOS) monoclonal antibody (1:30 dilution), goat anti-$p22^{phox}$ polyclonal antibody (1:50 dilution), rabbit anti-angiotensin II (Ang II) serum (1:100 dilution) or rabbit anti-angiotensin type 1 receptor (AT_1R) polyclonal antibody (1:100 dilution) as the primary antibody. After the sections had been rinsed with phosphate-buffered saline (PBS), they were incubated for 1 h at room temperature with the second antibody (Alexa Fluor 488 anti-goat, anti-rabbit or anti-mouse IgG antibody; 1:5000 dilution in each case), followed by a wash with PBS. The fluorescence of Alexa Fluor 488 was then detected by confocal-laser-scanning microscopy, under identical conditions in each case. The fluorescence intensity of each image was read from eight randomly selected regions (10 × 10 pixels) and averaged using digital image analyser software (LSM5 PASCAL).

Frozen sections of LAD from LETO and OLETF rats were also stained with haematoxylin and eosin for morphometric analysis. Light-microscope images were recorded using a digital camera, and the wall thickness and number of smooth muscle cell nuclei across the wall were then measured using Scion Image software.

Western blot analysis

LAD strips were homogenized in sample buffer [62.5 mM Tris-HCl (pH 6.8), 10% glycerol and 2% sodium dodecyl sulfate (SDS)]. Western blotting was carried out according to a method described previously (Itoh *et al.*, 2003). An antibody against $p47^{phox}$ (1:200 dilution), $gp91^{phox}$ (1:200 dilution) or SOD (1:2000 dilution) was used as the primary antibody. The signals from the immunoreactive bands were detected by means of an enhanced chemiluminescence-detection system. The density of the protein was measured by densitometric scanning, as described previously (Itoh *et al.*, 2003).

Solutions

The composition of the Krebs solution was as follows (mM): 137.4 Na^+, 5.9 K^+, 1.2 Mg^{2+}, 2.6 Ca^{2+}, 15.5 HCO_3^-, 1.2 $H_2PO_4^-$, 134 Cl^- and 11.5 glucose. It was bubbled with 95% oxygen and 5% carbon dioxide (pH 7.3–7.4). The HEPES-buffered solution contained 99 mM NaCl, 4.7 mM KCl, 1.9 mM $CaCl_2$, 1.2 mM $MgSO_4$, 20 mM HEPES, 1.03 mM K_2HPO_4, 25 mM $NaHCO_3$ and 11.1 mM glucose, and its pH was 7.4. The PBS solution contained 2.9 mM NaH_2PO_4, 9 mM Na_2HPO_4 and 137 mM NaCl, and its pH was 7.2–7.4.

Drugs and materials

The drugs used were as follows: ACh-HCl, Daiichi-Sankyo Co. (Tokyo, Japan); L-NNA, charybdotoxin and apamin, Peptides Institute Inc. (Osaka, Japan); PEG-SOD and diclofenac sodium, Sigma Chemical Co. (St. Louis, MO, USA); L-012 and catalase (from bovine liver), Wako Pure Chemical Ind. (Osaka, Japan); guanethidine, Tokyo Kasei (Tokyo, Japan); DAF-2 diacetate, Daiichi Pure Chemicals (Tokyo, Japan); dihydroethidium, Molecular Probes (Eugene, OR, USA); L-NAME, Dojindo Lab. (Kumamoto, Japan); sevoflurane, Maruishi Pharmaceutical Co. (Osaka, Japan). Pravastatin sodium was kindly provided by Daiichi-Sankyo Co., and STA_2 by Ono Pharmaceutical Co. (Osaka, Japan).

Dihydroethidium was dissolved in dimethylsulphoxide to make a stock solution. All other drugs were dissolved in ultrapure Milli-Q water (Japan Millipore Corp., Tokyo, Japan). The stock solutions were stored at –80°C and diluted in Krebs or HEPES-buffered solution.

Tail-cuff plethysmograph (BP-98A), Softron (Tokyo, Japan); Antsense II, Horiba Ltd. (Kyoto, Japan); DCA2000 analyser, Siemens Medical Solutions Diagnostics (Tokyo, Japan); ELISA insulin kit, Shibayagi (Gunma, Japan); NOA 280, Sievers Instrument Inc. (Boulder, CO, USA); luminometer (Multibiolumat LB 9505C), Berthold (Bad Wildbad, Germany); OCT compound, Tissue Tek (SAKURA Finetechnical, Tokyo, Japan); confocal-laser-scanning microscope system (LSM5 PASCAL), Carl Zeiss (Jena, Germany); digital image-analyser software, Scion Image software (Scion Corp., Frederick, MD, USA); MAS-coated glass slides, Matsunami Glass (Kishiwada, Japan); anti-eNOS monoclonal antibody, BD Biosciences (San Jose, CA, USA); goat anti-$p22^{phox}$ polyclonal antibody and rabbit anti-AT_1R polyclonal antibody, Santa Cruz Biotechnology (Santa Cruz, CA, USA); rabbit anti-Ang II serum, Peninsula Laboratories (Belmont, CA, USA); Alexa Fluor 488 anti-goat, anti-rabbit or anti-mouse IgG antibody; Molecular Probes (Eugene, OR, USA); digital camera, Olympus (Tokyo, Japan); antibody against $p47^{phox}$, Santa Cruz Biotechnology; $gp91^{phox}$, BD Transduction Laboratories (Franklin Lakes, NJ, USA) or SOD, Stressgen (Ann Arbor, MI, USA); enhanced chemiluminescence-detection system, SuperSignal West Pico (Pierce, Rockford, IL, USA).

Statistical analysis

All results are expressed as mean ± SEM, with *n* values representing the number of rats used (each rat provided only one segment for a given experiment). A one-way or two-way ANOVA, with *post hoc* comparisons made using the Scheffé procedure or Student's unpaired *t*-test, was used for the statistical analysis. The level of significance was set at $P < 0.05$.

Results

General features of OLETF rat

As shown in Table 1, body weight was significantly higher in OLETF rats than in LETO rats but systolic blood pressure did not differ between these two groups. The concentrations of fasting blood glucose, HbA1c and serum insulin, and the HOMA-IR score, were all higher in OLETF rats than in LETO rats. The integrated blood glucose concentration within the first 2 h after oral glucose administration (estimated from the area under the curve, $AUC_{glucose}$) was significantly higher in OLETF rats than in LETO rats. The plasma NOx (NO_2^- + NO_3^-) concentration was not significantly different between the two groups. Following *in vivo* administration of pravastatin to OLETF rats, the blood glucose and serum insulin concentrations were normalized (to levels not different from those in control LETO rats) and the blood HbA1c level and HOMA-IR score were each significantly reduced (compared with those in pravastatin-untreated OLETF rats; $P < 0.05$). Neither body weight nor $AUC_{glucose}$ was altered by this pravastatin treatment (Table 1).

Superoxide production and NAD(P)H oxidase

Superoxide production (estimated from L-012 chemiluminescence intensity) in endothelium-intact LAD was significantly

Table 1 General features of the rat groups, LETO, OLETF and pravastatin-treated OLETF (OLETF + PRV)

	LETO (n)	*OLETF (n)*	*OLETF + PRV (n)*
Body weight (g)	523 ± 8 (17)	634 ± 16** (17)	639 ± 17** (11)
Systolic blood pressure (mm Hg)	144 ± 2 (5)	154 ± 3 (5)	154 ± 4 (5)
Blood glucose (mM)	8.5 ± 0.5 (17)	12.4 ± 0.9** (17)	9.9 ± 0.6 (11)
HbA1c (%)	2.9 ± 0.0 (17)	5.2 ± 0.3** (17)	4.1 ± 0.3**† (11)
Insulin (ng·mL^{-1})	2.3 ± 0.6 (11)	6.6 ± 1.1** (9)	4.4 ± 0.9 (9)
HOMA-IR score	19.6 ± 5.0 (11)	81.0 ± 12.6** (9)	48.7 ± 6.3**† (9)
Plasma NOx (μM)	35.0 ± 4.7 (9)	34.6 ± 2.9 (9)	36.1 ± 4.1 (9)
$AUC_{glucose}$ (mM·2 h)	768 ± 67 (4)	1976 ± 331** (4)	1519 ± 139** (4)

(*n*) indicates the number of animals used. Values are mean ± SEM. ANOVA: *$P < 0.05$, **$P < 0.01$ versus LETO; †$P < 0.05$ versus OLETF.
$AUC_{glucose}$, area under the curve within 2 h after oral glucose administration; LETO, Long-Evans Tokushima Otsuka rats; OLETF, Otsuka Long-Evans Tokushima Fatty rats; HbA1c, glycated haemoglobin A1c; HOMA-IR, homeostasis model assessment of insulin resistance; NOx, nitrite/nitrate.

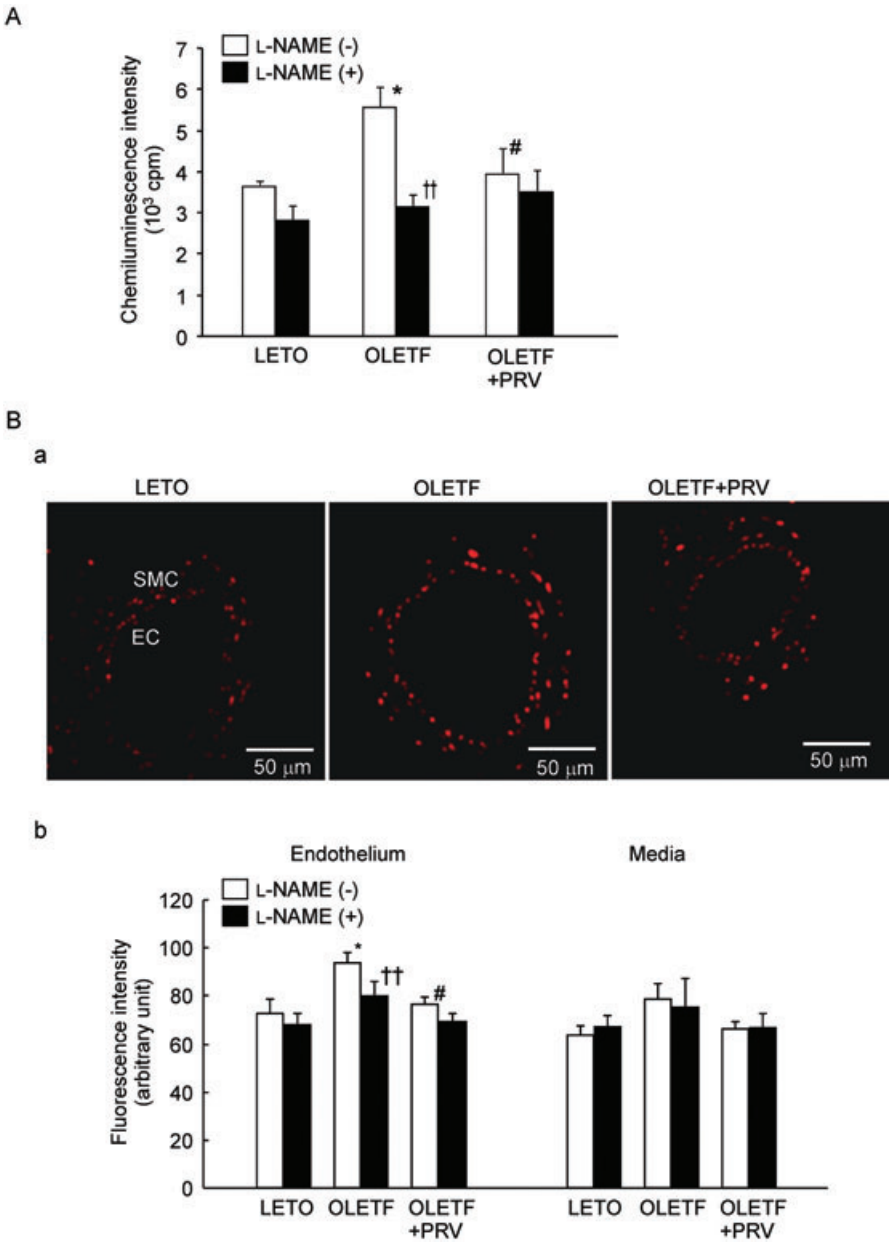

Figure 1 Superoxide production in left anterior descending coronary artery. (A) Chemiluminescence intensity of the superoxide-sensitive dye L-012 and the effect of N$^{\omega}$-nitro-L-arginine methyl ester (L-NAME) (3 mM). LETO Long-Evans Tokushima Otsuka rat; OLETF Otsuka Long-Evans Tokushima Fatty rat; OLETF + PRV, pravastatin-treated OLETF rat. Each column is the mean of data from four different preparations (from four different animals) with SEM. *$P < 0.05$ versus LETO. #$P < 0.05$ versus OLETF. ††$P < 0.01$ versus L-NAME (–). (Ba) Fluorescence intensity of the superoxide-sensitive dye dihydroethidium. SMC, smooth muscle cell; EC, endothelial cell. (Bb) Effect of L-NAME. Each column is the mean of data from five different sections (each from a different animal) with SEM. *$P < 0.05$ versus LETO. #$P < 0.05$ versus OLETF. ††$P < 0.01$ versus L-NAME (–).

higher in OLETF rats than in both LETO and pravastatin-treated OLETF rats (Figure 1A). Superoxide production was detected, by measuring ethidium fluorescence, in both the endothelial and medial regions of the vascular wall in all three groups of rats, and a significantly elevated level was found only in the *endothelial* region in OLETF rats (vs. both LETO and pravastatin-treated OLETF rats; Figure 1B). In each of the experiments where superoxide was measured, L-NAME (3 mM, an inhibitor of NOS-dependent superoxide production) (Xia *et al.*, 1998; Mata-Greenwood *et al.*, 2006) attenuated the increased superoxide production seen in OLETF rats (for L-012 chemiluminescence, Figure 1A; for ethidium fluorescence, Figure 1B).

The immunoreactive fluorescence against the NAD(P)H oxidase component p22^{phox} protein was distributed in both endothelial and medial regions in all three groups of rats (Figure 2A). The intensity in each region was higher in OLETF rats than in LETO rats, and the increased fluorescence in the endothelial region was significantly reduced by pravastatin treatment. The protein expressions of two other NAD(P)H oxidase components (p47^{phox} and gp91^{phox}) were also higher in OLETF rats than in LETO rats, and these were normalized by

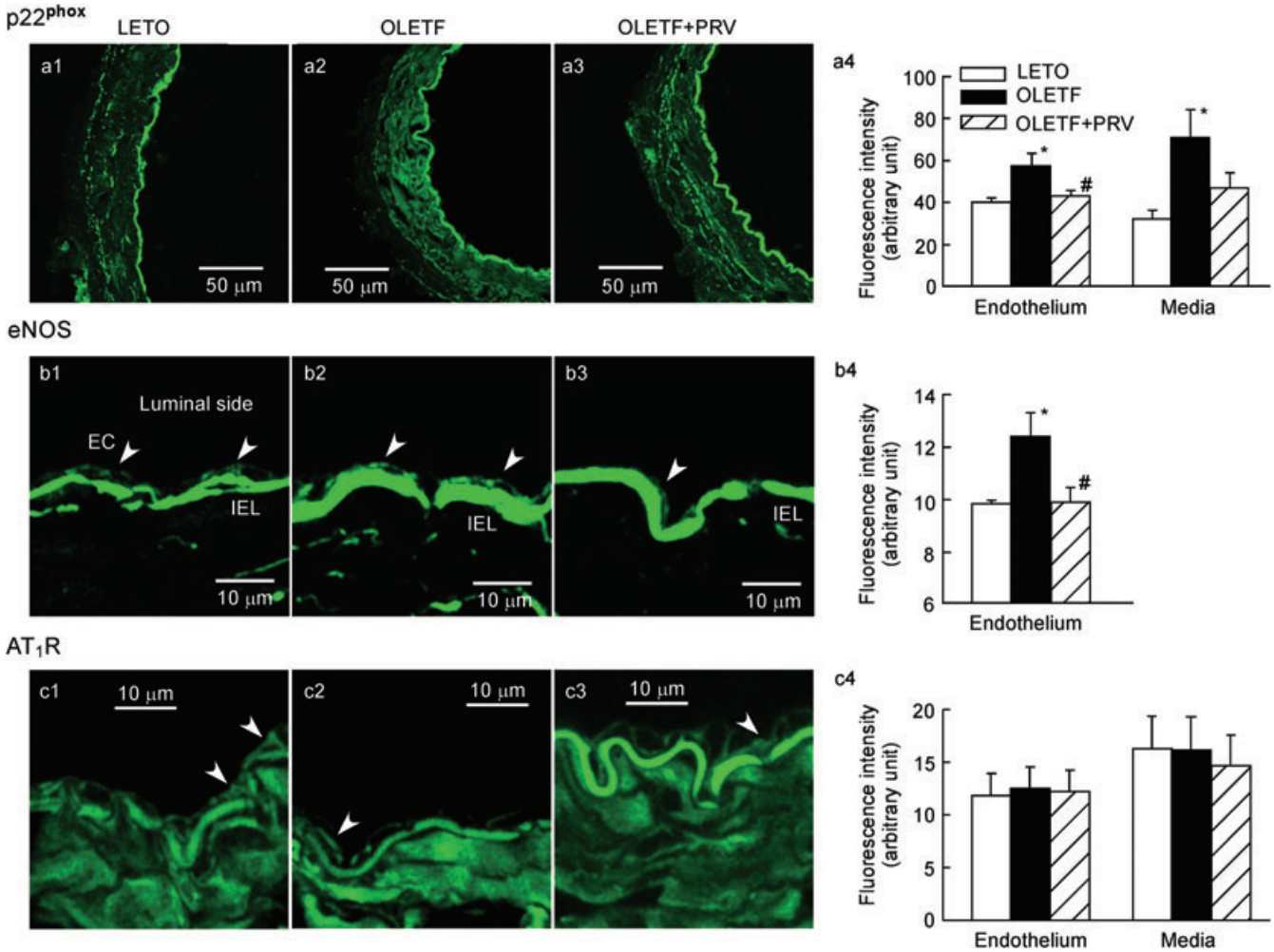

Figure 2 Immunostaining for p22^{phox}, endothelial NO synthase (eNOS) and angiotensin type 1 receptor (AT_1R) in left anterior descending coronary artery. Immunofluorescence staining against p22^{phox} (a), eNOS (b) and AT_1R (c) in preparations from a Long-Evans Tokushima Otsuka (LETO) rat (left column), an Otsuka Long-Evans Tokushima Fatty (OLETF) rat (middle column) and a pravastatin-treated OLETF (OLETF + PRV) rat (right column). EC, endothelial cell; IEL, internal elastic lamina. Arrowheads indicate endothelial cells. Similar observations were made in other sections obtained from five preparations, each from a different animal, in each group. (a4-c4) Summary of data from each group. Data are shown as mean ± SEM. *$P < 0.05$ versus LETO. *$P < 0.05$ versus LETO. #$P < 0.05$ versus OLETF.

pravastatin treatment (Figure 3A). The protein expression of the anti-oxidant Cu/Zn-SOD was similar among the three groups of rats (Figure 3B). The activity of NADPH oxidase was significantly higher in OLETF rats than in LETO rats, and it was normalized by pravastatin treatment (Figure 3C).

eNOS expression and NO production

Immunoreactivity against eNOS protein was detected (as fluorescence) only in the endothelial region in the three groups of rats, and it was significantly greater in OLETF rats than in either LETO or pravastatin-treated OLETF rats (Figure 2B). The NO production (estimated from the DAF-2 fluoresence) induced by ACh (10 μM) in the endothelial cells of LAD was similar among the three groups of rats (n = 4, $P > 0.05$; Figure 4).

Ang II and AT_1R expressions

Immunoreactive fluorescence signals against Ang II and AT_1R were detected in both the endothelial and medial regions of the LAD vascular wall in all three groups of rats. No significant differences in the protein expressions of Ang II (see below) and AT_1R (Figure 2C) in the endothelial and medial regions were detected between LETO rats and OLETF rats, with or without pravastatin treatment. In arbitrary units, the fluorescence intensities against Ang II in the endothelial region were 5.0 ± 0.9 (n = 5), 5.6 ± 1.2 (n = 5) and 5.4 ± 1.0 (n = 5) in LETO rats, OLETF rats and pravastatin-treated OLETF rats, respectively ($P > 0.05$ in each case), while those in the medial region were 7.9 ± 1.3, 8.6 ± 1.9 and 7.7 ± 1.1 respectively ($P > 0.05$ in each case).

Contractions induced by STA_2 and high K^+

Neither vascular wall thickness nor the number of smooth muscle cells across the wall in LAD was significantly different between LETO and OLETF rats (Figure 5A). High-K^+ (80 mM) and STA_2 (30 nM) each induced a contraction in endothelium-intact strips, and for each agent the maximum tensions were similar between LETO rats and OLETF rats

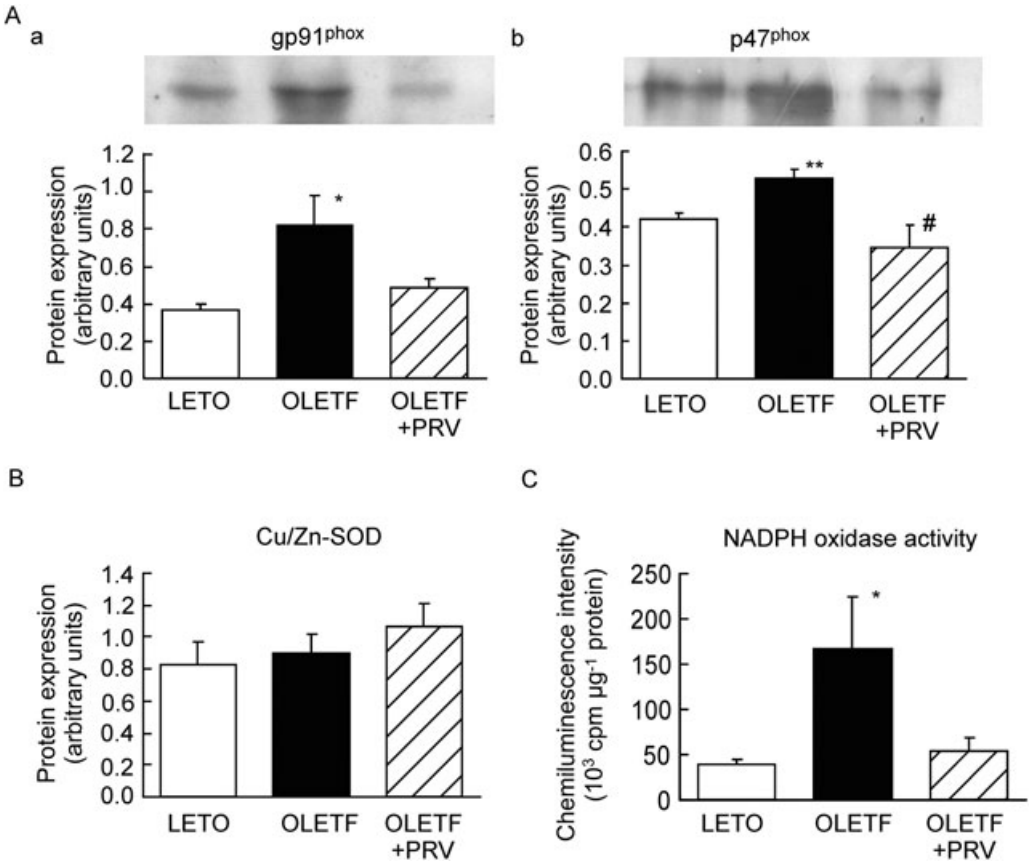

Figure 3 Expressions of nicotinamide adenine dinucleotide (phosphate) [NAD(P)H] oxidase components (gp91^{phox} and p47^{phox}) and Cu/Zn-SOD proteins, and nicotinamide adenine dinucleotide phosphate (NADPH) oxidase activity in left anterior descending coronary artery. (A) Protein expressions of gp91^{phox} (a) and p47^{phox} (b) were measured by western blot analysis. LETO Long-Evans Tokushima Otsuka rat; OLETF Otsuka Long-Evans Tokushima Fatty rat; OLETF + PRV, pravastatin-treated OLETF rat. (B) Expression of Cu/Zn- superoxide dismutase (SOD). (C) NADPH oxidase activity was measured in homogenized preparations. Each column is the mean of data from four different preparations (each from a different animal) with SEM. *$P < 0.05$, **$P < 0.01$ versus LETO. #$P < 0.05$ versus OLETF.

regardless of whether or not pravastatin had been administered (Figure 5B and C). The NOS inhibitor L-NNA (0.1 mM) enhanced the contraction induced by 30 nM STA_2 in endothelium-intact strips, the magnitude of the enhancement being similar among the three groups of rats discussed previously (Figure 5C).

ACh-induced relaxation

ACh (10^{-9}–10^{-6} M) induced a concentration-dependent relaxation of the contraction induced by 40 mM K^+ in endothelium-intact LAD strips that was similar between LETO rats and OLETF rats regardless of whether or not pravastatin had been administered (in each case, $P > 0.05$ by two-way-repeated ANOVA; Figure 6A). The pD2 (–log EC_{50}) values were 6.80 ± 0.10, 6.89 ± 0.16 and 6.98 ± 0.28 in LETO rats, OLETF rats and pravastatin-treated OLETF rats, respectively ($P > 0.5$ by one-way ANOVA), and those for E_{max} were 0.386 ± 0.036, 0.578 ± 0.083 and 0.637 ± 0.090 ($P > 0.05$ by one-way ANOVA) respectively.

PEG-SOD (100 u·mL^{-1}) plus catalase (400 u·mL^{-1}) significantly enhanced the ACh-induced relaxation of the high-K^+ contraction in OLETF rats ($n = 5$, $P < 0.05$) but not in either LETO or pravastatin-treated OLETF rats (in each case, $n = 5$, $P > 0.1$). ACh (10^{-9}–10^{-6} M) did not induce a relaxation of the high K^+-contraction in endothelium-*denuded* strips from either LETO or OLETF rats (data not shown).

ACh (10^{-9}–10^{-6} M) induced a concentration-dependent relaxation of the contraction induced by STA_2 (30 nM) in endothelium-intact strips that was similar among the three groups of rats (Figure 6B). No ACh-induced relaxation of the STA_2-contraction was observed in endothelium-*denuded* strips from either LETO or OLETF rats (data not shown).

Because L-NNA (0.1 mM) enhanced the contraction induced by STA_2 (30 nM) (Figure 5C), the concentration of STA_2 was reduced to 5 nM in the presence of L-NNA so as to match, as closely as possible, the amplitude of the STA_2-induced contraction obtained before application of L-NNA. In the presence of L-NNA, ACh (10^{-9}–10^{-6} M) induced a concentration-dependent relaxation of the contraction induced by STA_2 (5 nM) in endothelium-intact strips that was similar among the three groups of rats (Figure 6C).

ACh-induced smooth muscle cell hyperpolarization

The resting membrane potential of smooth muscle cells in endothelium-intact LAD strips from LETO rats was –46.4 ± 2.4 mV ($n = 6$), and ACh (1 µM) induced a hyperpolarization

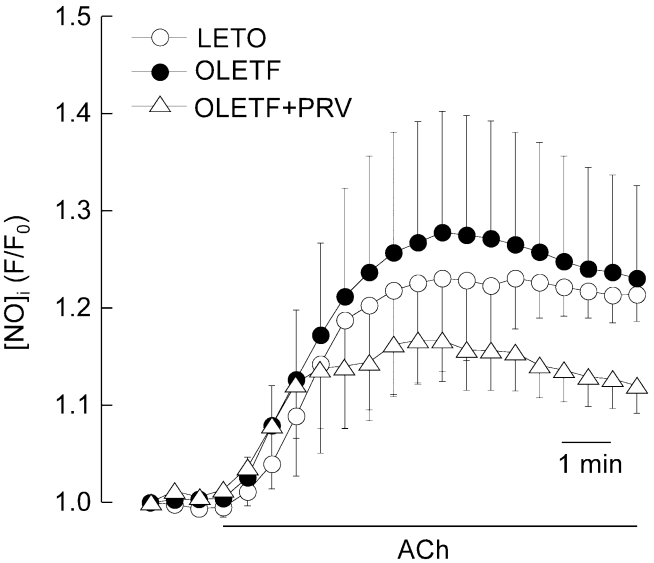

Figure 4 ACh-induced nitric oxide (NO) production in endothelial cells in left anterior descending coronary artery. Intracellular concentrations of NO ($[NO]_i$), as estimated from fluorescence-intensity changes in the NO-sensitive dye DAF-2. $[NO]_i$ is expressed as the ratio of F (fluorescence intensity at a given time after ACh-application) to F_0 (just before ACh-application). ACh (10 μM) was applied as indicated by the bar. Data are the mean from four different preparations (each from a different animal) with SEM. No significant differences were observed among the three groups of rats. LETO, Long-Evans Tokushima Otsuka; OLETF, Otsuka Long-Evans Tokushima Fatty, OLETF + PRV, pravastatin-treated OLETF.

(16.5 ± 1.6 mV, $n = 6$) (Figure 7A). No ACh-induced hyperpolarization was observed in endothelium-*denuded* strips from LETO rats (–2.0 ± 2.6 mV, $n = 3$). In endothelium-intact strips from LETO rats, L-NNA (0.1 mM) did not modify either the resting membrane potential (–47.6 ± 4.5, $n = 3$) or the ACh-induced hyperpolarization (17.5 ± 1.9 mV, $n = 3$; $P > 0.05$ before L-NNA application). In the presence of L-NNA, charybdotoxin (0.1 μM) + apamin (0.1 μM) did not affect the resting membrane potential (–49.4 ± 5.6 mV) but blocked the ACh-induced hyperpolarization (–4.3 ± 2.6 mV, $n = 3$; Figure 7A).

The resting membrane potential of smooth muscle cells in endothelium-intact strips from OLETF rats was –45.1 ± 2.3 mV ($n = 5$), and ACh (1 μM) induced a hyperpolarization (21.6 ± 2.8 mV, $n = 5$), these values being not significantly different from those obtained in LETO rats ($P > 0.05$ in each case; Figure 7). In the presence of L-NNA, ACh (1 μM) still induced a hyperpolarization (23.5 ± 0.3 mV, $n = 3$), and charybdotoxin (0.1 μM) + apamin (0.1 μM) blocked it (–2.8 ± 1.6 mV, $n = 3$; Figure 7B).

Discussion and conclusions

OLETF rats at 28 weeks of age were obese and mildly hyperglycaemic, with a relatively high serum insulin concentration in the fasting state (vs. age-matched LETO rats), as originally found by Kawano *et al*. (1992). In such rats, superoxide production was increased in LAD. However, the following endothelium-dependent responses were not significantly altered: (i) the ACh-induced relaxation of the high-K^+ contraction; (ii) the enhancement of the STA_2-contraction induced by the NO synthase inhibitor L-NNA; and (iii) the production of NO induced by ACh. These results indicate that both the spontaneous and the ACh-stimulated NO-release functions are normal in the LAD of OLETF rats. In addition, we are the first to demonstrate that the ACh-induced endothelium-dependent smooth muscle cell hyperpolarization and relaxation observed in the presence of L-NNA + diclofenac (i.e. the EDHF function) are also normal in this artery in OLETF rats.

Endothelial function and vascular superoxide production

Accumulating evidence indicates that the increased vascular superoxide production present in diabetic animals may lead to a dysfunction of endothelium-derived NO through the formation of peroxynitrite (inactivation of NO) and the induction of 'eNOS uncoupling' (via oxidation of the eNOS co-factor tetrahydrobiopterin) (Vásquez-Vivar *et al*., 1998; Fleming and Busse, 2003; Cai *et al*., 2005; Förstermann and Münzel, 2006). It has been suggested that activation of NAD(P)H oxidase is the most prominent mechanism underlying such an increase in vascular superoxide production *in vitro* as well as *in vivo* (Griendling *et al*., 1994; Rajagopalan *et al*., 1996; Kim *et al*., 2002). Further, it is thought that enhanced activity of the renin-angiotensin system and/or an increase in the expression of AT_1R protein may play a significant causal role in this effect on NAD(P)H oxidase, leading ultimately to the development of atherosclerosis and cardiovascular diseases (Nickenig and Murphy, 1996; Harrison, 1997; Nickenig *et al*., 1997). We found that in LAD obtained from OLETF rats at the early hyperglycaemic stage: (i) superoxide production was increased in endothelial cells (but not in smooth muscle cells); (ii) the protein expressions of the NAD(P)H oxidase components $p22^{phox}$, $p47^{phox}$ and $gp91^{phox}$, but not of either the amount of local Ang II or the expression of AT_1R protein, were increased; (iii) the activity of NADPH oxidase itself was increased; (iv) the protein expression of the anti-oxidant enzyme Cu/Zn-SOD was not altered; and (v) a very high concentration of L-NAME [an inhibitor of superoxide production via 'uncoupled eNOS' (Xia *et al*., 1998; Mata-Greenwood *et al*., 2006)] attenuated the endothelial superoxide production. In addition, we had previously found that the selective NAD(P)H oxidase inhibitor apocynin (but not the mitochondrial respiratory chain uncoupler rotenone) completely blocked the elevated superoxide production observed in aortae isolated from OLETF rats at the same stage (Kikuchi *et al*., 2008). Collectively, the above results indicate that in OLETF rats at the early hyperglycaemic stage: (i) there is enhanced NAD(P)H oxidase activity within endothelial cells in the LAD and this causes a small increase in superoxide production, which (ii) induces 'eNOS uncoupling', leading to a larger increase in superoxide production. These steps are not related to any change in either the amount of local Ang II or AT_1R protein expression in this artery. We also found that unlike the endothelial cells, the smooth muscle cells showed no increase in superoxide production, although $p22^{phox}$ protein expression was enhanced. This suggests that in addition to an increased NAD(P)H oxidase activity, certain other changes (such as the formation of 'uncoupled eNOS' within the endothelial cells) are needed for an increase in superoxide

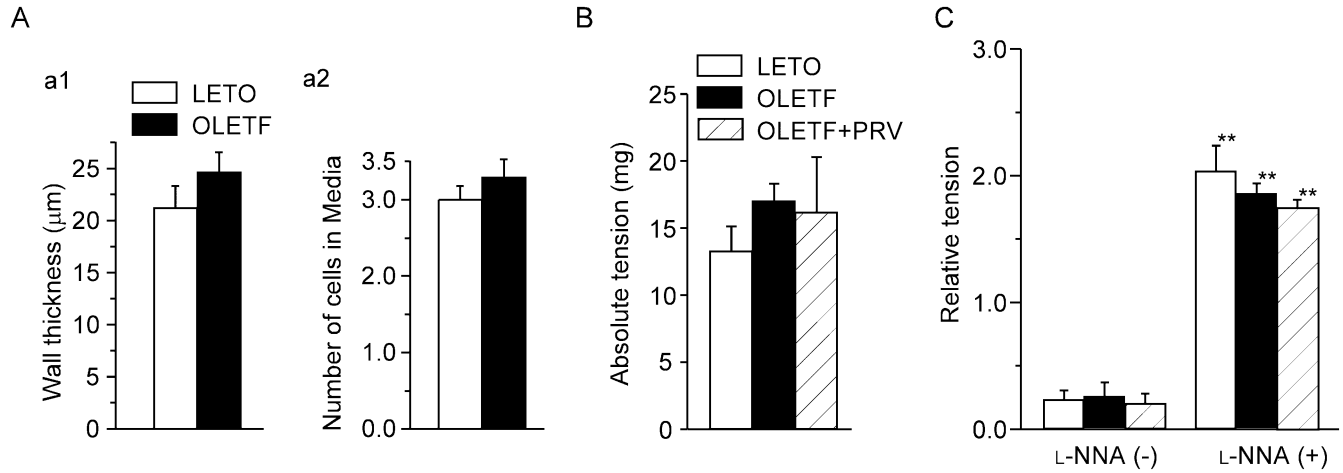

Figure 5 Morphometric characteristics and the effects of high-K^+ and 9,11-epithio-11,12-methano-thromboxane A_2 (STA_2) on mechanical activities. (A) Summaries of left anterior descending coronary artery (LAD) wall thickness (a1) and number of smooth muscle cells across the wall (a2) in Long-Evans Tokushima Otsuka (LETO) rats and Otsuka Long-Evans Tokushima Fatty (OLETF) rats. Summary of data obtained for absolute tension induced by 80 mM K^+ (B) and effect of the nitric oxide synthase inhibitor N^{ω}-nitro-L-arginine (L-NNA) on STA_2 (30 nM)-induced contractions in endothelium-intact strips of LAD (C). LETO: LETO rats; OLETF: OLETF rats; OLETF + PRV: pravastatin-treated OLETF rats. In (C), the maximum amplitude of contraction induced by 80 mM K^+ before application of L-NNA was normalized as a relative tension of 1.0. Data are shown as mean ± SEM for four strips, each from a different animal, in each group. $^{**}P < 0.01$ versus corresponding L-NNA (–).

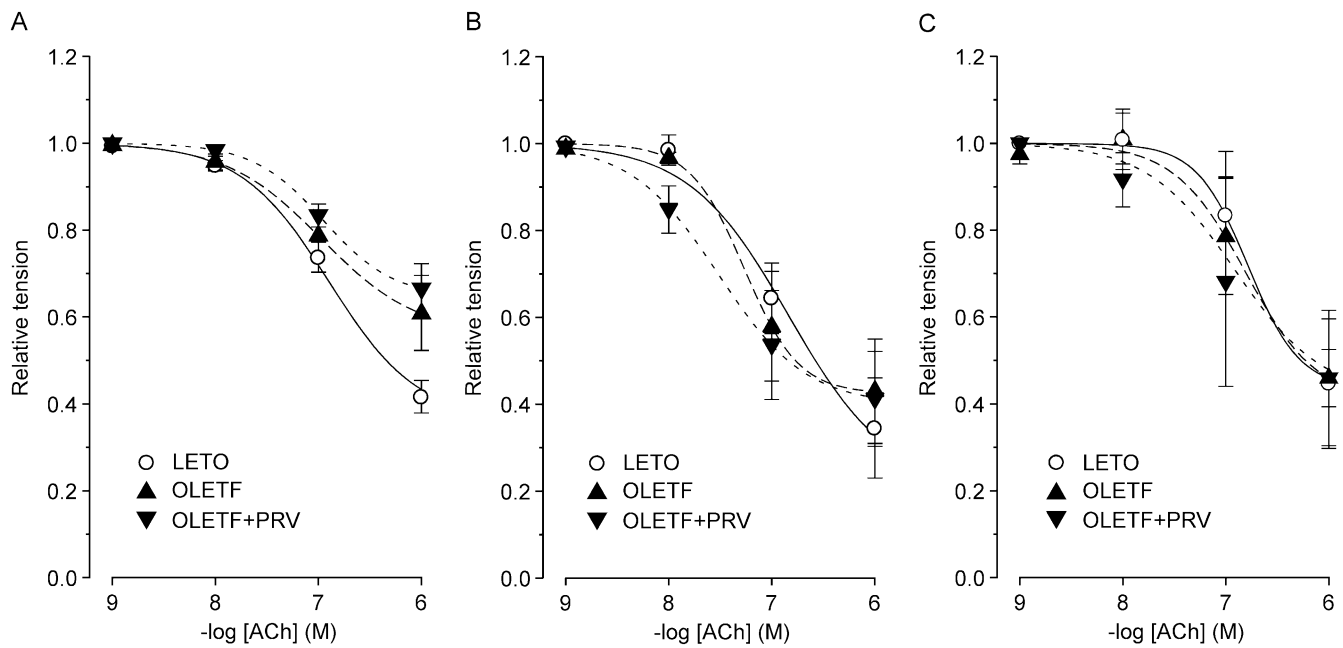

Figure 6 ACh-induced relaxation of the contractions induced by high K^+ and 9,11-epithio-11,12-methano-thromboxane A_2 (STA_2). Concentration-response relationships for ACh-induced relaxations in endothelium-intact strips of left anterior descending coronary artery from Long-Evans Tokushima Otsuka (LETO) rats, Otsuka Long-Evans Tokushima Fatty (OLETF) rats and pravastatin-treated OLETF rats (OLETF + PRV) in the presence of the cyclooxygenase inhibitor diclofenac, (A) on the contraction induced by 40 mM K^+, (B) on the contraction induced by 30 nM STA_2, (C) on the contraction induced by 5 nM STA_2 in the presence of N^{ω}-nitro-L-arginine (0.1 mM). Means of 3–5 strips, each from a different animal, in each group, with SEM shown by vertical bar.

production to occur in the smooth muscle cells in the LAD of OLETF rats at the early hyperglycaemic stage.

It is thought that in several animal models of type 1 or type 2 diabetes, the elevated blood glucose level leads to an increase in vascular superoxide production, thereby causing a dysfunction of endothelium-derived NO in conduit arteries (De Vriese *et al.*, 2000). It has recently been suggested that insulin resistance correlates with coronary endothelial dysfunction in humans (Balletshofer *et al.*, 2000; Quiñones *et al.*, 2004; Prior *et al.*, 2005). In the present experiments, we used the 28-week-old OLETF rat as our model. This model exhibits mild hyperglycaemia with a high blood insulin concentration, and so it is unclear whether the increased superoxide production we observed was secondary to the hyperglycaemia or to the insulin resistance. This remains to be clarified in future work.

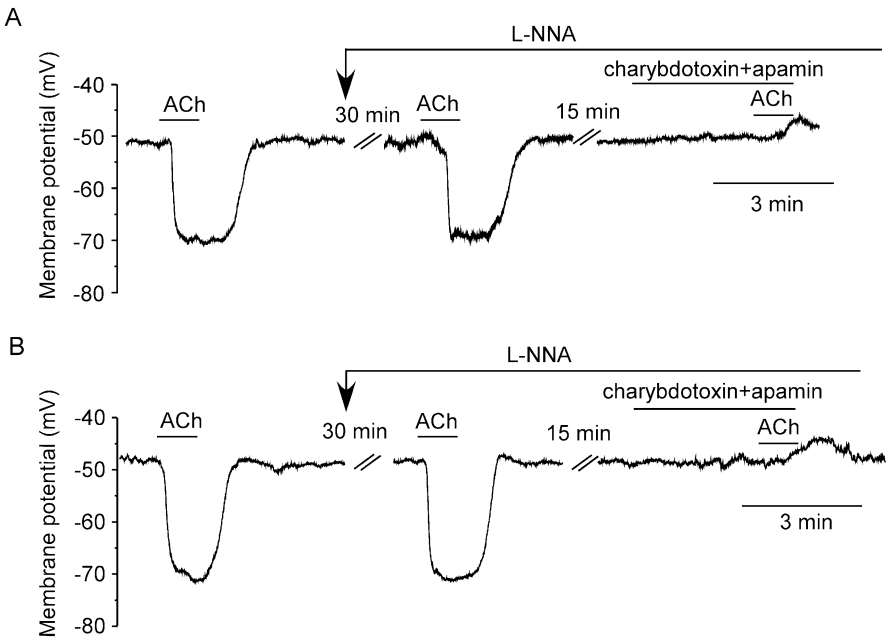

Figure 7 Effects of N^{ω}-nitro-L-arginine (L-NNA) and blockers of Ca^{2+}-activated K^{+}-channels on ACh-induced smooth muscle cell hyperpolarization. The experiments were performed in the presence of the cyclooxygenase inhibitor diclofenac. Representative tracings of the effects of L-NNA (0.1 mM), in the presence or absence of charybdotoxin (0.1 μM) + apamin (0.1 μM), on ACh-induced smooth muscle cell hyperpolarization in left anterior descending coronary artery from Long-Evans Tokushima Otsuka rat (A) and Otsuka Long-Evans Tokushima Fatty rat (B).

Endothelium-derived NO and EDHF are each important for the regulation by the endothelium of vasomotor function in coronary arteries (Kugiyama *et al.*, 1997; De Vriese *et al.*, 2000). It might be anticipated that an enhanced vascular superoxide production would cause a dysfunction of endothelium-derived NO (Vásquez-Vivar *et al.*, 1998; Fleming and Busse, 2003; Cai *et al.*, 2005; Förstermann and Münzel, 2006). However, we found that in OLETF rats at the early hyperglycaemic stage, both ACh-induced endothelial NO production and the contraction-regulating function of NO were normal in the LAD despite an increased superoxide production. This does not accord with findings previously made in *aortae* from type 2 diabetic animals, including OLETF rats (Sakamoto *et al.*, 1998; Kagota *et al.*, 2000; Kim *et al.*, 2002; Minami *et al.*, 2002). These results may reflect differences in the development of endothelial dysfunction among different vascular regions during the early hyperglycaemic stage of diabetes under conditions of increased vascular superoxide production. We also found that under these conditions, eNOS protein expression in LAD was increased in the OLETF rat (a result consistent with a previous finding; Jesmin *et al.*, 2002) and, moreover, that combined application of PEG-SOD (the membrane-permeable SOD) plus catalase (to break down the H_2O_2 produced by PEG-SOD) enhanced the ACh-induced NO-mediated relaxation in OLETF rats, but not in either LETO or pravastatin-treated OLETF rats. These results suggest that a portion of the increased eNOS that is not 'uncoupled' helps to maintain the function of endothelium-derived NO in LAD in OLETF rats at the early hyperglycaemic stage.

In the presence of L-NNA + diclofenac, the ACh-induced endothelium-dependent smooth muscle cell hyperpolarization in LAD was the same in our OLETF rats as in the control LETO rats. The hyperpolarization was inhibited by the combined application of the intermediate-conductance K_{Ca}-channel inhibitor charybdotoxin and the small-conductance K_{Ca}-channel inhibitor apamin (agents that are well-established inhibitors of EDHF) (Félétou and Vanhoutte, 2000). Moreover, the ACh-induced, endothelium-dependent relaxation observed in the presence of L-NNA + diclofenac was not different between OLETF rats and LETO rats. These results indicate that in LAD, the function of EDHF is also retained in OLETF rats at the early hyperglycaemic stage. The above results are in contrast to findings made in mesenteric arteries obtained from OLETF rats at this stage (Minami *et al.*, 2002). We previously found in rabbits that under conditions of increased endothelial superoxide production, the modulation of ACh-induced endothelium-dependent hyperpolarization differs between aortic valves (Kusama *et al.*, 2005a) and middle cerebral arteries (Watanabe *et al.*, 2008). Thus, taken as a whole, the results available at present suggest that the ability of superoxide to down-regulate the function of EDHF may differ among different types of vascular beds in animals at the early hyperglycaemic stage of diabetes.

Effects of pravastatin on vascular superoxide production

In this study, pravastatin was administered *in vivo* to OLETF rats for 8 weeks starting at 20 weeks of age, and this treatment significantly reduced the fasting blood HbA1c concentration. Because there was only a slight (and not significant) decrease in the serum insulin concentration, the HOMA-IR score was significantly decreased. These results indicate that pravastatin induces a partial recovery of the decrease in

sensitivity to insulin shown by the target organs in OLETF rats, when it is administered once hyperglycaemia has already developed. Under such conditions, endothelial superoxide production in LAD was normalized, together with reductions not only in the protein expressions of NAD(P)H oxidase components ($p22^{phox}$, $p47^{phox}$ and $gp91^{phox}$) but also in NADPH oxidase activity. In addition, pravastatin reduced the eNOS protein expression in this artery to the normal level, it was an unexpected result because various HMG-CoA reductase inhibitors have been found to increase eNOS protein or mRNA expression in endothelial cells (Laufs and Liao, 1998; Wagner *et al*., 2000). Further, pravastatin inhibited the development of 'eNOS uncoupling' [as estimated from the action of L-NAME (an inhibitor of superoxide production by 'uncoupled eNOS')] in the LAD of OLETF rats. Interestingly, 'eNOS uncoupling' has been found to be more profound when eNOS protein is overexpressed under conditions of increased vascular superoxide production in Apo-E-knockout mice (Takaya *et al*., 2007). Collectively, the above results suggest that in OLETF rats at the early hyperglycaemic stage, pravastatin normalizes not only the raised eNOS protein expression, but also 'eNOS uncoupling' in the LAD, possibly by inhibiting NAD(P)H oxidase. A recent clinical study in Japan indicated that pravastatin reduces the risk of coronary heart disease in patients who have hypercholesterolaemia but no history of coronary heart disease or stroke (Nakamura *et al*., 2006). The usefulness of HMG-CoA reductase inhibitors for the secondary prevention of cardiovascular diseases has also been demonstrated in diabetic patients with (Pyorälä *et al*., 1997) and without (Sacks *et al*., 2002) hypercholesterolaemia. Thus, it seems likely that in coronary arteries in type 2 diabetes, the inhibition of vascular superoxide production induced by pravastatin may make a significant contribution to the normalization of endothelial functions that is seen with this agent (Sacks *et al*., 2002) and thereby help to reduce the adverse cardiovascular events associated with this disease state.

We conclude that because superoxide production is increased and 'eNOS uncoupling' has developed, the endothelial cells are in a pathophysiological state in the LAD of OLETF rats at the early hyperglycaemic stage (although the function of NO is not critically modified, possibly because of additional NO derived from the enhanced expression of eNOS). It may be that the existence of such a state in the endothelial cells increases the likelihood of endothelial dysfunction developing in the future. Because pravastatin can evidently inhibit all these changes in endothelial cells, we suggest that this agent may prevent or retard the development of endothelial dysfunction in coronary arteries in type 2 diabetes by inhibiting endothelial superoxide production.

Acknowledgements

We thank Dr RJ Timms for a critical reading of the manuscript. This work was partly supported by a Grant-In-Aid for Scientific Research from Japan Society for the Promotion of Science.

Conflict of interest

None.

References

Balletshofer BM, Rittig K, Enderle MD, Volk A, Maerker E, Jacob S *et al*. (2000). Endothelial dysfunction is detectable in young normotensive first-degree relatives of subjects with type 2 diabetes in association with insulin resistance. *Circulation* **101**: 1780–1784.

Bayraktutan U, Draper N, Lang D, Shah AM (1998). Expression of functional neutrophil-type NADPH oxidase in cultured rat coronary microvascular endothelial cells. *Cardiovasc Res* **38**: 256–262.

Bonow RO, Bohannon N, Hazzard W (1996). Risk stratification in coronary artery disease and special populations. *Am J Med* **101**: 4A17S–22S; discussion 22S–24S.

Cai S, Khoo J, Channon KM (2005). Augmented BH_4 by gene transfer restores nitric oxide synthase function in hyperglycemic human endothelial cells. *Cardiovasc Res* **65**: 823–831.

Cash D, Beech JS, Rayne RC, Bath PM, Meldrum BS, Williams SC (2001). Neuroprotective effect of aminoguanidine on transient focal ischaemia in the rat brain. *Brain Res* **905**: 91–103.

Chen Y, Ohmori K, Mizukawa M, Yoshida J, Zeng Y, Zhang L *et al*. (2007). Differential impact of atorvastatin versus pravastatin on progressive insulin resistance and left ventricular diastolic dysfunction in a rat model of type II diabetes. *Circ J* **71**: 144–152.

De Vriese AS, Verbeuren TJ, Van de Voorde J, Lameire NH, Vanhoutte PM (2000). Endothelial dysfunction in diabetes. *Br J Pharmacol* **130**: 963–974.

Félétou M, Vanhoutte PM (2000). Endothelium-dependent hyperpolarization of vascular smooth muscle cells. *Acta Pharmacol Sin* **21**: 1–18.

Fleming I, Busse R (2003). Molecular mechanisms involved in the regulation of the endothelial nitric oxide synthase. *Am J Physiol Regul Integr Comp Physiol* **284**: R1–R12.

Förstermann U, Münzel T (2006). Endothelial nitric oxide synthase in vascular disease: from marvel to menace. *Circulation* **113**: 1708–1714.

Freeman DJ, Norrie J, Sattar N, Neely RD, Cobbe SM, Ford I *et al*. (2001). Pravastatin and the development of diabetes mellitus: evidence for a protective treatment effect in the West of Scotland Coronary Prevention Study. *Circulation* **103**: 357–362.

Garland CJ, Plane F, Kemp BK, Cocks TM (1995). Endothelium-dependent hyperpolarization: a role in the control of vascular tone. *Trends Pharmacol Sci* **16**: 23–30.

Griendling KK, Minieri CA, Ollerenshaw JD, Alexander RW (1994). Angiotensin II stimulates NADH and NADPH oxidase activity in cultured vascular smooth muscle cells. *Circ Res* **74**: 1141–1148.

Halcox JP, Schenke WH, Zalos G, Mincemoyer R, Prasad A, Waclawiw MA *et al*. (2002). Prognostic value of coronary vascular endothelial dysfunction. *Circulation* **106**: 653–658.

Harrison DG (1997). Endothelial function and oxidant stress. *Clin Cardiol* **20**: II-11–II-17.

Itoh T, Kajikuri J, Kuriyama H (1992). Characteristic features of noradrenaline-induced Ca^{2+} mobilization and tension in arterial smooth muscle of the rabbit. *J Physiol* **457**: 297–314.

Itoh T, Kajikuri J, Tada T, Suzuki Y, Mabuchi Y (2003). Angiotensin II-induced modulation of endothelium-dependent relaxation in rabbit mesenteric resistance arteries. *J Physiol* **548**: 893–906.

Jesmin S, Sakuma I, Hattori Y, Fujii S, Kitabatake A (2002). Long-acting calcium channel blocker benidipine suppresses expression of angiogenic growth factors and prevents cardiac remodelling in a Type II diabetic rat model. *Diabetologia* **45**: 402–415.

Kagota S, Yamaguchi Y, Nakamura K, Kunitomo M (2000). Altered endothelium-dependent responsiveness in the aortas and renal

arteries of Otsuka Long-Evans Tokushima Fatty (OLETF) rats, a model of non-insulin-dependent diabetes mellitus. *Gen Pharmacol* **34**: 201–209.

Kannel WB, McGee DL (1979). Diabetes and glucose tolerance as risk factors for cardiovascular disease: the Framingham study. *Diabetes Care* **2**: 120–126.

Kawano K, Hirashima T, Mori S, Saitoh Y, Kurosumi M, Natori T (1992). Spontaneous long-term hyperglycemic rat with diabetic complications. Otsuka Long-Evans Tokushima Fatty (OLETF) strain. *Diabetes* **41**: 1422–1428.

Kikuchi C, Kajikuri J, Watanabe Y, Itoh T (2008). Effect of chronic administration of pravastatin on enhanced vascular superoxide production in a type 2 diabetes rat model. *Nagoya Med J* **49**: 95–110.

Kim YK, Lee MS, Son SM, Kim IJ, Lee WS, Rhim BY *et al*. (2002). Vascular NADH oxidase is involved in impaired endothelium-dependent vasodilation in OLETF rats, a model of type 2 diabetes. *Diabetes* **51**: 522–527.

Kugiyama K, Ohgushi M, Motoyama T, Sugiyama S, Ogawa H, Yoshimura M *et al*. (1997). Nitric oxide-mediated flow-dependent dilation is impaired in coronary arteries in patients with coronary spastic angina. *J Am Coll Cardiol* **30**: 920–926.

Kusama N, Kajikuri J, Watanabe Y, Suzuki Y, Katsuya H, Itoh T (2005a). Characteristics of attenuated endothelium-dependent relaxation seen in rabbit intrapulmonary vein following chronic nitroglycerine administration. *Br J Pharmacol* **145**: 193–202.

Kusama N, Kajikuri J, Yamamoto T, Watanabe Y, Suzuki Y, Katsuya H *et al*. (2005b). Reduced hyperpolarization in endothelial cells of rabbit aortic valve following chronic nitroglycerine administration. *Br J Pharmacol* **146**: 487–497.

Laufs U, Liao JK (1998). Post-transcriptional regulation of endothelial nitric oxide synthase mRNA stability by Rho GTPase. *J Biol Chem* **273**: 24266–24271.

Marchenko SM, Sage SO (1996). Calcium-activated potassium channels in the endothelium of intact rat aorta. *J Physiol* **492**: 53–60.

Mata-Greenwood E, Jenkins C, Farrow KN, Konduri GG, Russell JA, Lakshminrusimha S *et al*. (2006). eNOS function is developmentally regulated: uncoupling of eNOS occurs postnatally. *Am J Physiol Lung Cell Mol Physiol* **290**: L232–L241.

Matthews DR, Hosker JP, Rudenski AS, Naylor BA, Treacher DF, Turner RC (1985). Homeostasis model assessment: insulin resistance and beta-cell function from fasting plasma glucose and insulin concentrations in man. *Diabetologia* **28**: 412–419.

Minami A, Ishimura N, Harada N, Sakamoto S, Niwa Y, Nakaya Y (2002). Exercise training improves acetylcholine-induced endothelium-dependent hyperpolarization in type 2 diabetic rats, Otsuka Long-Evans Tokushima fatty rats. *Atherosclerosis* **162**: 85–92.

Nakamura H, Arakawa K, Itakura H, Kitabatake A, Goto Y, Toyota T *et al*. (2006). Primary prevention of cardiovascular disease with pravastatin in Japan (MEGA Study): a prospective randomised controlled trial. *Lancet* **368**: 1155–1163.

Nakamura T, Houchi H, Minami A, Sakamoto S, Tsuchiya K, Niwa Y *et al*. (2001). Endothelium-dependent relaxation by cilostazol, a phosphodiesterase III inhibitor, on rat thoracic aorta. *Life Sci* **69**: 1709–1715.

Nickenig G, Murphy TJ (1996). Enhanced angiotensin receptor type 1 mRNA degradation and induction of polyribosomal mRNA binding proteins by angiotensin II in vascular smooth muscle cells. *Mol Pharmacol* **50**: 743–751.

Nickenig G, Jung O, Strehlow K, Zolk O, Linz W, Schölkens BA *et al*. (1997). Hypercholesterolemia is associated with enhanced angiotensin AT_1-receptor expression. *Am J Physiol* **272**: H2701–2707.

Prior JO, Quiñones MJ, Hernandez-Pampaloni M, Facta AD, Schindler TH, Sayre JW *et al*. (2005). Coronary circulatory dysfunction in insulin resistance, impaired glucose tolerance, and type 2 diabetes mellitus. *Circulation* **111**: 2291–2298.

Pyorälä K, Pedersen TR, Kjekshus J, Faergeman O, Olsson AG, Thorgeirsson G (1997). Cholesterol lowering with simvastatin improves prognosis of diabetic patients with coronary heart disease. A subgroup analysis of the Scandinavian Simvastatin Survival Study (4S). *Diabetes Care* **20**: 614–620.

Quiñones MJ, Hernandez-Pampaloni M, Schelbert H, Bulnes-Enriquez I, Jimenez X, Hernandez G *et al*. (2004). Coronary vasomotor abnormalities in insulin-resistant individuals. *Ann Intern Med* **140**: 700–708.

Quyyumi AA (1998). Endothelial function in health and disease: new insights into the genesis of cardiovascular disease. *Am J Med* **105**: 32S–39S.

Rajagopalan S, Kurz S, Münzel T, Tarpey M, Freeman BA, Griendling KK *et al*. (1996). Angiotensin II-mediated hypertension in the rat increases vascular superoxide production via membrane NADH/NADPH oxidase activation. Contribution to alterations of vasomotor tone. *J Clin Invest* **97**: 1916–1923.

Sacks FM, Tonkin AM, Craven T, Pfeffer MA, Shepherd J, Keech A *et al*. (2002). Coronary heart disease in patients with low LDL-cholesterol: benefit of pravastatin in diabetics and enhanced role for HDL-cholesterol and triglycerides as risk factors. *Circulation* **105**: 1424–1428.

Sakamoto S, Minami K, Niwa Y, Ohnaka M, Nakaya Y, Mizuno A *et al*. (1998). Effect of exercise training and food restriction on endothelium-dependent relaxation in the Otsuka Long-Evans Tokushima Fatty rat, a model of spontaneous NIDDM. *Diabetes* **47**: 82–86.

Shepherd J, Cobbe SM, Ford I, Isles CG, Lorimer AR, MacFarlane PW *et al*. (1995). Prevention of coronary heart disease with pravastatin in men with hypercholesterolemia. West of Scotland Coronary Prevention Study Group. *N Engl J Med* **333**: 1301–1307.

Takaya T, Hirata K, Yamashita T, Shinohara M, Sasaki N, Inoue N *et al*. (2007). A specific role for eNOS-derived reactive oxygen species in atherosclerosis progression. *Arterioscler Thromb Vasc Biol* **27**: 1632–1637.

Vásquez-Vivar J, Kalyanaraman B, Martásek P, Hogg N, Masters BS, Karoui H *et al*. (1998). Superoxide generation by endothelial nitric oxide synthase: the influence of cofactors. *Proc Natl Acad Sci USA* **95**: 9220–9225.

Wagner AH, Köhler T, Rückschloss U, Just I, Hecker M (2000). Improvement of nitric oxide-dependent vasodilatation by HMG-CoA reductase inhibitors through attenuation of endothelial superoxide anion formation. *Arterioscler Thromb Vasc Biol* **20**: 61–69.

Watanabe Y, Kusama N, Itoh T (2008). Effects of chronic in vivo administration of nitroglycerine on ACh-induced endothelium-dependent relaxation in rabbit cerebral arteries. *Br J Pharmacol* **153**: 132–139.

Xia Y, Tsai AL, Berka V, Zweier JL (1998). Superoxide generation from endothelial nitric-oxide synthase. A Ca^{2+}/calmodulin-dependent and tetrahydrobiopterin regulatory process. *J Biol Chem* **273**: 25804–25808.

Yamamoto T, Kajikuri J, Watanabe Y, Suzuki Y, Suzumori K, Itoh T (2005). Chronic nitroglycerine administration reduces endothelial nitric oxide production in rabbit mesenteric resistance artery. *Br J Pharmacol* **146**: 534–542.

Yu Y, Ohmori K, Chen Y, Sato C, Kiyomoto H, Shinomiya K *et al*. (2004). Effects of pravastatin on progression of glucose intolerance and cardiovascular remodeling in a type II diabetes model. *J Am Coll Cardiol* **44**: 904–913.